Journal of Southeast University (English Edition) Dec. 2001 Vol.17 No.2 ISSN 1003—7985

# Structure Analysis of Wheel Torque Transducer

Bassam Al Mohdi* Zhang Weigong

(Department of Instrument Science and Engineering, Southeast University, Nanjing 210096, China)

**Abstract:** This paper describes the finite element modeling and analysis of torque transducer, which commonly uses force sensor's strain gauge's distribution, by using the ANSYS software. The main work in this article is to build the finite element model of the sensor structure's elastic body, analyze the boundary conditions when the elastic body is loaded by the driving moment $M_y$ and displaying the result.

**Key words:** torque transducer, finite element, ANSYS software

Possessing the ability to test vehicle in a completely virtual environment has been the dream of many engineers. In China, for instance, the automobile industry has been developing rigorously as the pillar of the country's mechanical industry. Large automobile plants are gradually shifting their production focus with imported technologies. Analysis and study of the performance of vehicles become more and more important in developing new models. At present, the research of vehicle's performance is mainly operated through real vehicle tests and computer simulations. The torque transducer used here is capable of acquiring several types of data such as forces, torque, data for test procedures and information on field usage of vehicles. The measurement of wheel torque transducer can reflect the effects of the driving system and braking system on the wheel while the vehicle running. The measuring range can be very wide (rotating speed 0 – 3?000?r/m, driving moment – 10 – 10?kN · m)[1].

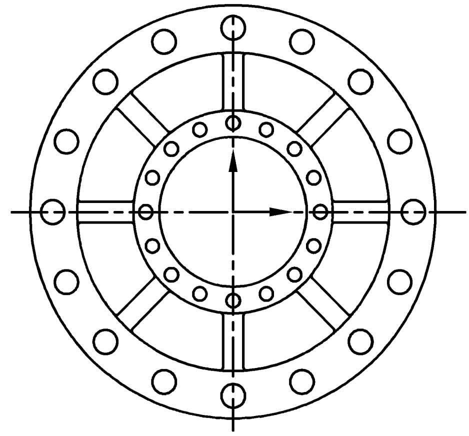

**Fig.1** Structure of elastic body

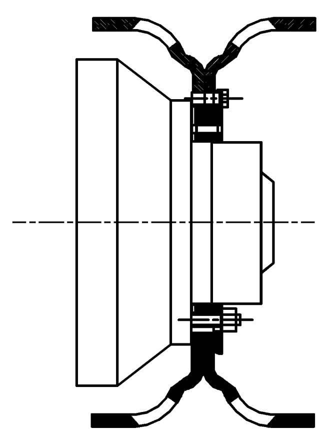

**Fig.2** Installation of torque transducer on the vehicle's wheel

## 1 The Strain Gauge of Elastic Body with Simple Structure

The elastic body doesn't need transitional flange when connected to the wheel hub and wheel rim as shown in Fig.1. Thus, the wheel installed with the transducer is guaranteed basically of no deviation from the original position. Meanwhile there will be slight additional weight and the installation is simple as shown in Fig.2[1].

The distribution of strain gauge is of great significance in the transducer design. Reasonable distribution not only can simplify the structure of the transducer's elastic body, but also effectively eliminate the errors and interference as well as increase the accuracy of the transducer's measurement. The strain gauge foils are located on both sides of the deformation girder of the elastic body with a good adhesion as illustrated in Fig.3[1].

The four-arm complete-bridge method can be adopted to constitute the bridge of strain gauge foils as shown in Fig.4(a) and simplify it to the bridge in Fig. 4(b) under the function of the driving moment. The supplying and outputing voltage must be transmitted contact-free to and from the bridge by configuration such as that illustrated in Fig.5[2].

Received 2001 – 01 – 18.

* Born in 1969, male, master, Syria.

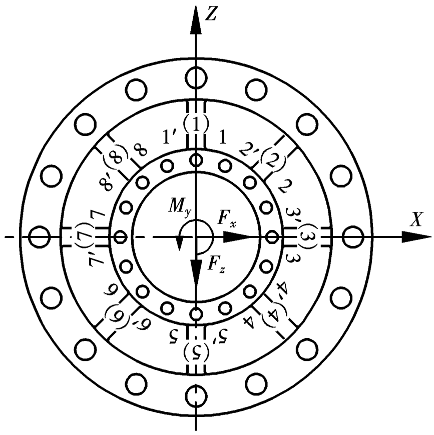


**Fig**. 3 Distribution of elastic body

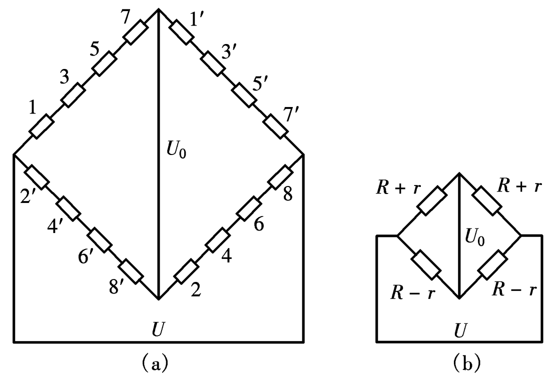


**Fig**.4 Strain gauge

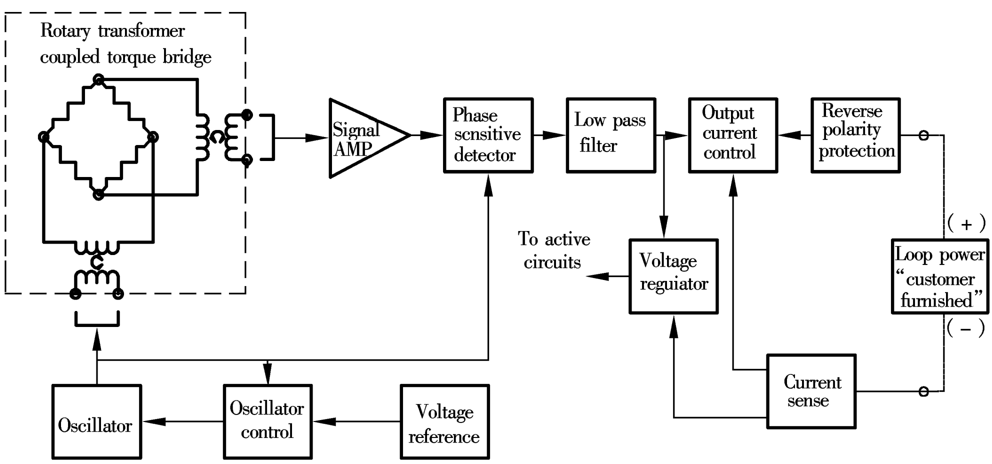


**Fig**.5 The configuration of transmitted contact-free system

The standard method to evaluate the torque transducer is using a static calibration. The torque transducer is typically fixed to a frame or other fixtures for the purpose of applying a calibrated load[3].

In this article, the structure of torque transducer's elastic body will be studied by using finite element method with ANSYS software. This study includes: build the geometric model, analyze the elastic body's strain girders in order to obtain the results of deforming shape, DOF solutions, stresses, strains and then plot the results and graphics.

## 2 Description of ANSYS Software

There is always a contradiction between the elastic body structure design and the strain gauge distribution in the design of the force sensor. Direct output of the force sensor is of great importance in solving this contradiction and the decoupling as well as in developing a simple structure.

The design of the elastic body's structure is complicated with large numbers of strain gauges. It is also difficult to analyze the effects of the force and moment on the elastic girder. The ANSYS program has a progressively high ability to solve these problems[1,2].

The ANSYS software includes sets of manuals that provide descriptions of the procedures, elements, and theoretical details. It also gives a brief description to build a finite element model, apply load to the model, obtain solutions and review the results, design optimization and sub-modeling, structure analysis (e.g. a static analysis, harmonic, transient dynamic, …) and thermal analysis, etc.

## 3 Solid Model of Elastic Body

In creating the solid model of elastic body, the CAD system is used, as it's recommended. The solid work software is used directly to create and build the solid model of elastic body, and then imported the model into ANSYS as shown in Fig.6.

Then, the model can be meshed just as one can do for any model created in ANSYS. As illustrated in Fig.7, repairing and enhancing the topological and geometric models is a very interactive process in ANSYS.

The ANSYS program provides a much more intuitive method for importing and repairing solid models. After meshing the model, it will appear slightly different, because the small geometric features contain tiny lines, which require small element sizes for proper discretization. However, these small

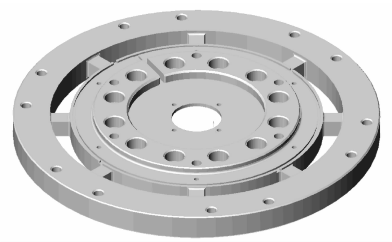

**Fig**.6 Solid model of elastic body

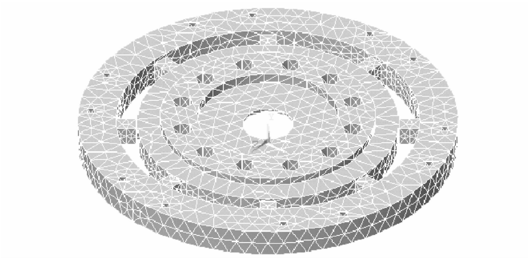

**Fig**.7 Repairing and meshing solid model

geometric features are not usually significant when determining the overall stress in the part when subjected to loads. Thus, we can assume that the features are not necessary for the analysis and defeuture the model before meshing and solving.

## 4 Analysis of the Finite Element Model

In this analysis, the "solid92" element type has been used, which has a quadratic displacement behavior and is well suited to model irregular meshes (such as produced from various CAD/CAM systems) as shown in Fig.7. The element is defined by ten nodes having three degrees of freedom at each node: translations in the nodal $X$, $Y$, and $Z$ directions. the "solid93" also has been used, to add three DOF rotations about the nodes $X$, $Y$, and $Z$ directions, but will not be used in the solution. "Solid92" also has plasticity, creep, swelling, stress stiffening, large deflection and large strain capabilities. The geometry, node locations, and the coordinate system for this element are shown in Fig.8[4,5].

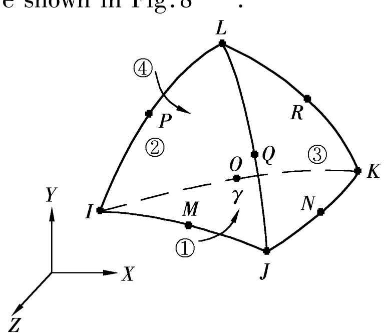


**Fig**.8 Solid92 tetrahedral structural

The output element stress directions are parallel to the element coordinate system as illustrated in Fig.9.

The boundary terms of elastic body are the interior and exterior holes that are dependent on elastic body's installation to the vehicle wheel. The exterior holes

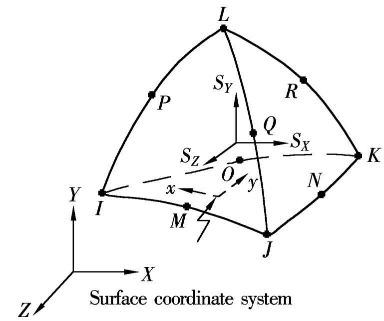


**Fig**.9 Solid92 stress output

have been chosen to apply the DOF constraints as an area constraint for all degrees of freedom $U_X$, $U_Y$, $U_Z$, $ROT_X$, $ROT_Y$ and $ROT_Z$, which is zero value for each DOF, while the interior holes of the model apply the forces and moments on nodes.

The analysis depends on applying the maximum value of the driving moment on the model ($M_y$ = 10?kN·m).

$$M_y = F \times R$$

where $R$ is the radius of the main circle of the interior holes ($R$ = 0.067?m); $F$ is the perpendicular force.

Because the structure is completely symmetric, then each hole bears ($\frac{M_y}{12} \approx$ 833?N·m).

$$F = \frac{833}{0.067} = 12?433?\mathrm{N}$$

The components of the force when its applied to the model are shown in Tab.1

**Tab**.1 List nodal forces for selected nodes

| Number | Node | $F_X$/N | $F_Z$/N | Number | Node | $F_X$/N | $F_Z$/N |
|---|---|---|---|---|---|---|---|
| 1 | 5?737 | 12?340 | 1?515 | 7 | 5?804 | – 12?340 | – 1?515 |
| 2 | 5?726 | 9?929 | 7?482 | 8 | 5?793 | – 9?929 | – 7?482 |
| 3 | 5?715 | 4?857 | 11?445 | 9 | 5?782 | – 4?857 | – 11?445 |
| 4 | 5?692 | – 1?515 | 12?340 | 10 | 5?765 | 1?515 | – 12?340 |
| 5 | 5?507 | – 7?482 | 9?929 | 11 | 5?759 | 7?482 | – 9?929 |
| 6 | 5?815 | – 11?445 | 4?857 | 12 | 5?748 | 11?445 | – 4?857 |

Fig.10 shows how the constraints and loads are applied onto the symmetric model.

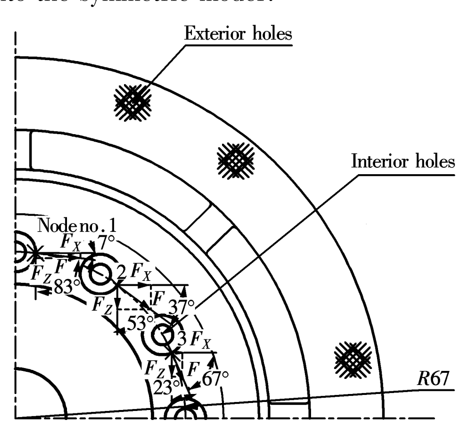


**Fig**.10 Applied forces and constraints to symmetric model

The input summary of the element is described in Tab.2, the material properties of which are related to the alloy steel "40CrNiMoA"[6-8].

**Tab**.2 Solid92 input summary

| | |
|---|---|
| Element name | Solid92 |
| Nodes | *I*, *J*, *K*, *L*, *M*, *N*, *O*, *P*, *Q*, *R* |
| Degree of freedom | "Translations" $U_X = U_Y = U_Z = 0$<br>"Rotating" $ROT_X = ROT_Y = ROT_Z = 0$ |
| Real constants | None |
| Material properties | "Young's modulus" $E_X = E_Y = E_Z =$ 210?kN/mm$^2$<br>"Poisson's ratio" $NU_{XY} = NU_{YZ} = NU_{XZ} = 0.3$<br>"Density"DENS = $7.8 \times 10^{-6}$kg/mm$^3$ |

## 5 Results

After analyzing the force transducer's elastic body, we can see the deformed and undeformed shape of the model when it was loaded in Fig.11.

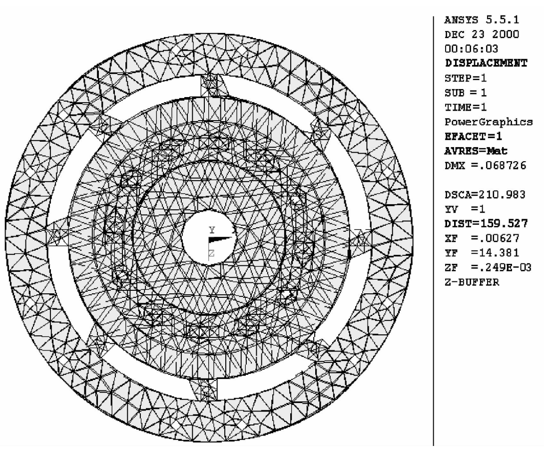


**Fig**.11 Deformed and undeformed

The output from the solution consists of the nodal solution (or the primary degree of freedom solution). The nodal solutions such as nodal displacements are calculated for all active degrees of freedom in the model, determined by union of all DOF labels associated with all the active element type.

The output listing of stress, and strain is given at the Centerior (or near center) of the element. The output quantities calculated as the average of the integration point values are shown in Fig.12 and Fig.13, respectively. In Fig.12, every color related to individual average value of stress over all the elastic body from minimum value up to maximum one with "N/mm$^2$" measurement unit.

From the stress distribution, it can be seen that the range of the stress contours changes from 0.342?917 – 906.372?N/mm$^2$.

From the strain distribution, it can also be seen the range of the strain contours changes from $0.212 \times 10^{-5}$ – 0.561?1 $\times 10^{-2}$.

Obviously, the most important and sensitive part in the (torque) force transducer is the girder, because the strain gauge foils are located on both sides of the

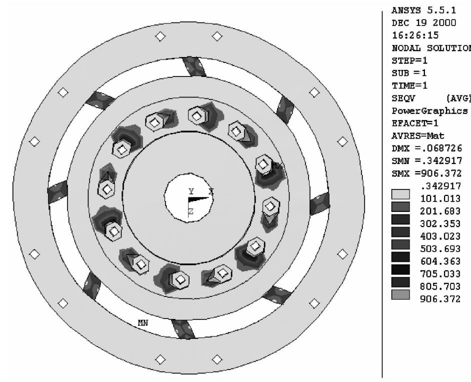


**Fig**.12 Stress solution

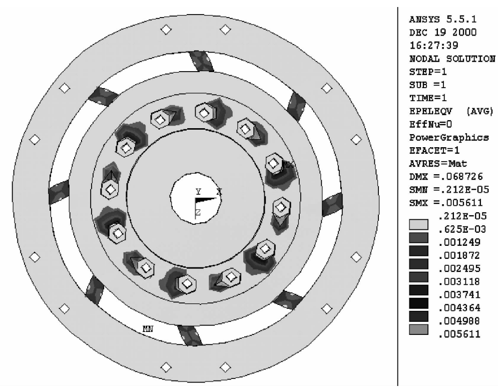


**Fig**.13 Strain elastic solution

deformation girder. Therefore, the output results must take deformation girder into consideration.

The transducer's symmetric structure enables us to take only one girder to get the results and solutions. Thus, we can choose the girder "3" to get the results through the six nodes attached to the girder. Every node related to a different color.

The locations *X*, *Y*, and *Z* of these nodes are shown in Tab.3.

**Tab**.3 List all selected nodes

| Node | *X*/mm | *Y*/mm | *Z*/mm | Color |
|---|---|---|---|---|
| 8?258 | 99.819 | 9.999 | 6.000 | Blue |
| 9?150 | 103.863 | 7.899 | 6.000 | Magenta |
| 9?097 | 105.108 | 16.999 | 6.000 | M-Red |
| 9?149 | 107.832 | 9.999 | 6.000 | M-Red |
| 9?151 | 111.838 | 7.900 | 6.000 | Red |
| 8?573 | 115.845 | 17.000 | 6.000 | Yellow |

The output nodal solution per nodal (DOF) of girder (nodal displacement results) is illustrated in Tab.4.

**Tab**.4 Nodal DOF listing

| Node | $U_X$/mm | $U_Y$/mm | $U_Z$/mm | $U_{SUM}$/mm |
|---|---|---|---|---|
| 8?258 | 0.262?98 $\times 10^{-2}$ | 0.234?99 $\times 10^{-2}$ | 0.391?15 $\times 10^{-1}$ | 0.392?74 $\times 10^{-1}$ |
| 9?150 | 0.729?06 $\times 10^{-2}$ | 0.194?33 $\times 10^{-2}$ | 0.316?07 $\times 10^{-1}$ | 0.324?95 $\times 10^{-1}$ |
| 9?097 | 0.113?20 $\times 10^{-2}$ | 0.133?83 $\times 10^{-2}$ | 0.296?79 $\times 10^{-1}$ | 0.297?36 $\times 10^{-1}$ |
| 9?149 | 0.934?57 $\times 10^{-2}$ | 0.103?87 $\times 10^{-2}$ | 0.229?88 $\times 10^{-1}$ | 0.248?37 $\times 10^{-1}$ |
| 9?151 | 0.82?396 $\times 10^{-2}$ | 0.403?12 $\times 10^{-3}$ | 0.141?65 $\times 10^{-1}$ | 0.163?92 $\times 10^{-1}$ |
| 8?573 | 0.386?98 $\times 10^{-2}$ | 0.152?81 $\times 10^{-2}$ | 0.493?93 $\times 10^{-2}$ | 0.645?81 $\times 10^{-2}$ |

Fig.14 presents the average of distribution output results of the displacements on the girder, the location of nodes, and node values, which are illustrated in Tab.4.

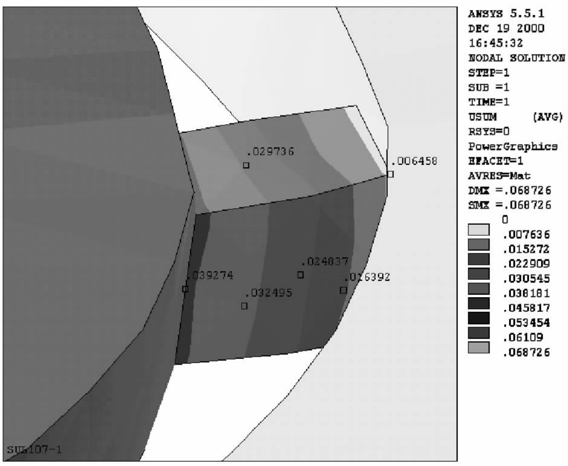


**Fig**.14 DOF results

From the displacement distribution, it can be seen that the range of the displacement contours changes from 0 – 0.687?26?mm over all the transducer.

The output nodal solution per nodes (Stress & Strain-Elastic) of girder for selected nodes is illustrated in Tab.5 and Tab.6, respectively.

**Tab**.5 Nodal stress listing N · mm$^{-2}$

| Node | $S_1$ | $S_2$ | $S_3$ | $S_{INT}$ | $S_{EQV}$ |
|---|---|---|---|---|---|
| 8?258 | 438.22 | 121.51 | 107.89 | 330.32 | 323.73 |
| 9?150 | 191.90 | 16.650 | 0.149?44 | 191.75 | 184.05 |
| 9?097 | 114.85 | – 3.856?0 | – 130.45 | 245.29 | 212.47 |
| 9?149 | 22.621 | 0.102?63 | – 0.942?13 | 23.563 | 23.095 |
| 9?151 | 9.175?5 | – 8.862?0 | – 106.85 | 116.03 | 108.14 |
| 8?573 | – 3.266?3 | – 42.278 | – 119.82 | 116.55 | 102.76 |

Fig.15 and Fig.16 present the locations of the selected nodes on the girder and the values of stress and elastic strain respectively.

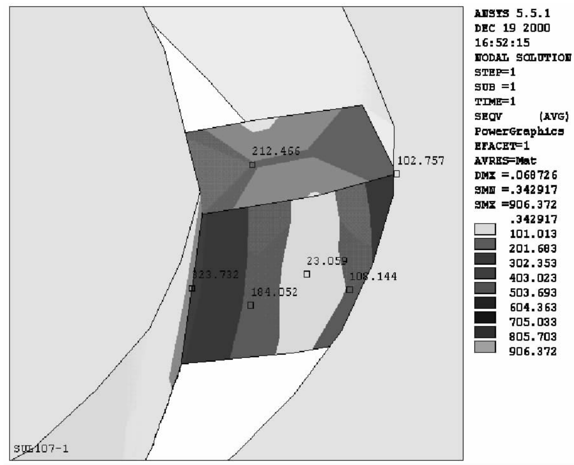


**Fig**.15 Nodal stress result for selected node

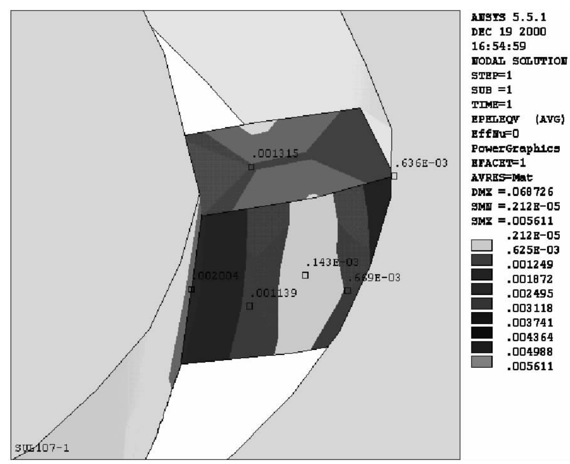


**Fig**.16 Nodal strain result for selected node

**Tab**.6 Nodal elastic strain listing

| Node | $EPEL_1$ | $EPEL_2$ | $EPEL_3$ | $EPEL_{INT}$ | $EPEL_{EQV}$ |
|---|---|---|---|---|---|
| 8?258 | 0.175?90 × $10^{-2}$ | – 0.201?55 × $10^{-3}$ | – 0.285?83 × $10^{-3}$ | 0.204?49 × $10^{-2}$ | 0.200?41 × $10^{-2}$ |
| 9?150 | 0.889?79 × $10^{-3}$ | – 0.195?06 × $10^{-3}$ | – 0.297?21 × $10^{-3}$ | 0.118?70 × $10^{-2}$ | 0.113?94 × $10^{-2}$ |
| 9?097 | 0.738?74 × $10^{-3}$ | 0.392?72 × $10^{-5}$ | – 0.779?74 × $10^{-3}$ | 0.151?85 × $10^{-2}$ | 0.131?53 × $10^{-2}$ |
| 9?149 | 0.108?92 × $10^{-3}$ | – 0.304?81 × $10^{-4}$ | – 0.369?49 × $10^{-4}$ | 0.145?87 × $10^{-3}$ | 0.142?74 × $10^{-3}$ |
| 9?151 | 0.209?00 × $10^{-3}$ | 0.973?39 × $10^{-3}$ | – 0.509?27 × $10^{-3}$ | 0.718?27 × $10^{-3}$ | 0.669?46 × $10^{-3}$ |
| 8?573 | 0.216?01 × $10^{-3}$ | – 0.254?92 × $10^{-4}$ | – 0.505?49 × $10^{-3}$ | 0.721?50 × $10^{-3}$ | 0.636?12 × $10^{-3}$ |

## 6 Conclusion

From the above analysis, it can be seen that the use of finite element ANSYS software in modeling and analyzing is very useful and convenient in analyzing the force transducer's elastic body under boundary conditions. The results given here will provide a basis for further analysis of the system.

From Tab.5 and Tab.6, it can be found out the minimum values of stress and elastic strain are 23.059? N/mm$^2$, 0.142?74 × $10^{-3}$, respectively, in node 9?149, which is the position near to the neutral layer of the symmetric girder. This allows to install the foil strain gauges around the node.

From Fig.15 and Fig.16, it can be seen that under the function of torque $M_y$, the load on every girder is $M_y/8$, so that the transformation of each girder is the same. Furthermore, according to every deforming girder, the position of the deforming sheet is symmetry, the transformation is the same or on the contrary. Thus, the deforming value of all sheets must be equal, suppose it to be $\varepsilon_M^1$.

The static performance of force sensor's strain gauge's distribution can be a feedback for the dynamic analysis, because the output stress results from the static performance will be the prestress condition in the dynamic transient analysis.

Furthermore, we can analyze the elastic strain body when subjected to load (force and moment) $F_x$, $F_y$, $F_z$, $M_x$, $M_z$ and $M_y$, respectively. This case will gives the ability to perform the six-degree-of-freedom force sensor's strain gauge's distribution analysis.

## References

1 W.G. Zhang and W.H.Qin, Research and application of wheel torque transducer, Journal of Southeast University (In Chinese), vol.29, no.6A, pp.6 – 9, 1999

2 E.Zbler, A.Dukart, F.Heintz, and Krohr, A non-contact strain gauge torque sensor for automotive servo driven steering system, *Sensor and Actuators A*, pp.39 – 46, 1994

3 L.Jodi, Sommerfeld, and Richard A. Meyer, Correlation and Accuracy of a wheel force transducer as developed and tested on a flat-trac, *SAE Technical Paper Series*, pp.1 – 7, 1999

4 K.J.Bathe, Finite Element Procedures in Engineering Analysis, Prentie-Hall and Englewood Cliffs, 1982

5 R.D.Cook, Concepts and Applications of Finite Element Analysis, (second edition), John Wiley and Sons, New York, 1981

6 B.Robert, Ross metallic materials specification handbook, pp. 570 – 582, 1980

7 J.R.An, X.Z.Jin, A book of commonly used metallic materials both at home and abroad, Standard Information Institute of Shaxi Province, pp.107 – 118, 1982

8 H.Shen, A book of mechanic engineering (In Chinese), 3th volume, Mechanic Industry Press House, Beijing, pp.12 – 105 1983

# 车轮扭矩传感器的结构分析

巴萨姆·阿尔·默赫迪　　张为公

（东南大学仪器科学与工程系，南京 210096）

**摘　要**　用 ANSYS 软件描述了有限元建模及扭矩传感器的分析,通常采用力传感器的应变片布片方案.本文主要工作是建立传感器结构的弹性体的有限元模型,分析滚动力矩 $M_y$ 作用于弹性体时的应力和应变分布情况,并展示结果.

**关键词**　扭矩传感器，有限元，ANSYS 软件

**中图分类号**　TH823